Solid Freeform Fabrication 2023: Proceedings of the 34th Annual International Solid Freeform Fabrication Symposium – An Additive Manufacturing Conference
Reviewed Paper

DEVELOPMENT OF HIGHLY FILLED BIO-BASED COMPOSITES FOR SUSTAINABLE, LOW-COST FEEDSTOCK: PROCESSING EFFECTS ON POROSITY AND FIBER ALIGNMENT

Katie Copenhaver[a], Meghan Lamm[a], Amber Hubbard[a]

[a]Manufacturing Science Division, Oak Ridge National Laboratory, Oak Ridge, TN, 37830.

Abstract

A poly(lactic acid) composite with a high loading of bio-based fibers was developed using a combination of high-aspect ratio (AR) wood pulp and low-AR wood flour along with viscosity modifiers to maximize mechanical performance, maintain processability, and lower the cost and embodied energy of the resulting feedstock. An optimized composite formulation containing 40 wt.% of a blend of high- and low-AR natural fibers with a rice bran-based wax processing aid was scaled up to produce pellet feedstock using twin screw extrusion, and materials were compression and injection molded to investigate the effect of fiber alignment on material performance. The feedstock was then printed on the Big Area Additive Manufacturing system at Oak Ridge National Laboratory. Print parameters including temperature gradients, screw and gantry speeds, layer times, and nozzle designs were varied to minimize sharkskinning, warpage, and porosity of the final parts. A strong effect of the nozzle size on the resulting porosity was observed, and consistent trends between decreasing porosity, increasing fiber alignment, and increasing mechanical performance were identified after printing with different nozzles, compression molding, and injection molding.

Introduction

Although interest in both additive manufacturing (AM) and sustainable feedstocks for manufacturing has rapidly increased in recent years, the high cost of many bio-based polymeric materials in comparison to petroleum-based commodity plastics continues to restrict their use. Large format additive manufacturing (LFAM) systems have also opened a variety of new applications areas for AM and new thermoplastic feedstocks as well.[1] Poly(lactic acid) (PLA) is a common feedstock for AM on small, desktop scales as well as LFAM systems and is currently one of the only completely bio-based thermoplastics available on a commercial scale.[2, 3] Discontinuous fibers or particles are often added to PLA and other resins to improve the mechanical properties of additively manufacture parts, add specific functionalities, or enable printability on larger scales.[4] The addition of natural fibers as opposed to synthetic to PLA also allows the composite to remain 100% bio-based and industrially biodegradable. Wood flour (WF) in particular is a popular filler for AM feedstock due to its low cost, and PLA/WF can be readily purchased as filament for AM from such retailers as Amazon.[5, 6] The Oak Ridge National Laboratory, along with other research institutions, have conducted numerous LFAM studies using PLA filled with 20 wt.% of WF, and most of the commercially available PLA/WF filament is

available at a filler loading of less than 20 wt.%.[7] However, these composites remain more expensive than commodity polymers such as polypropylene or polyethylene, but their performance (both mechanical and thermal) restricts their use in more demanding, higher value applications in which carbon fiber-reinforced composites are typically employed.[8] As such, this study aims to develop a lower-cost, bio-based composite feedstock for LFAM using higher loadings of natural fibers or particles and a small inclusion of additives for viscosity modification while retaining the mechanical performance of the composite. Various loadings of WF in PLA were first investigated to determine a qualitative maximum limit of filler. A second type of natural filler, bleached Kraft pulp fibers, was also investigated for its improved reinforcing potential in comparison to WF. Finally, different viscosity modifiers were considered in the highly loaded composite to enable processability of the final composite. An optimal formulation was then scaled up to produce a large batch of feedstock for LFAM. Samples were prepared using the resulting composite by additively manufacturing with different processing conditions as well as compression and injection molding. Finally, the effects of processing methods on the performance of the final composite were compared.

Materials and Methods

Materials

Poly (L-Lactide), herein referred to as PLA (Ingeo 4043D), was purchased from NatureWorks, LLC. Wood flour (WF, 100 mesh, softwood pine) was acquired from American Wood Fiber. Bleached Kraft pulp fibers (CreaTech TC750), herein referred to as Creafill, was acquired from Creafill Fibers Corp. Polyethylene glycol (PEG, 8000 g/mol) and poly(methyl acrylate-co-ethylene-co-glycidyl methacrylate) (P(MA-co-E-co-GMA)) were acquired from Sigma Aldrich. Wax flakes consisting of polyol fatty acids (Licolub WE 60FL) were acquired from Clariant AG.

Sample preparation (bench scale)

All materials were dried at 60 ℃ in a convection oven for a minimum of 4 hours before processing to remove moisture. Bench-scale samples were compounded using a melt mixer (Intelli-Torque Plasticorder half-size mixer, C. W. Brabender Instruments Inc.). PLA was first mixed at 180 ℃ for two minutes at 60 RPM, after which the desired additive (for some samples, PEG, PMA-co-E-co-GMA, or wax) was added and allowed to mix for another 3 minutes. The desired amount of WF and/or Creafill was then added and allowed to mix for a further 5 minutes. The content of WF was first varied from 20 to 50 wt.% in the PLA without additives. Ratios of Creafill and WF at 100/0, 75/25, 50/50, 25/75 (Creafill/WF) were then compounded in PLA at 40 wt.% total fiber content. Finally, Creafill/WF at a 75/25 ratio was compounded in PLA at 40 wt.% total fiber with PEG, P(MA-co-E-co-GMA), and wax additives at 1 wt.% (separately).

After compounding, each sample was compression molded into 1 mm films at 180 ℃ for 5 minutes using a hydraulic press (Carver). The films were then cut into approximately 3 mm strips and compression molded into uniform bars at 180 ℃ for 5 minutes following ASTM D4703. Bars were routed into ASTM D638 Type V dogbones using a router (Tensilkut). Neat PLA pellets were also compression molded to Type V dogbones using the same procedure.

Characterization (bench scale)

The torque during melt mixing of select samples was recorded as a function of time by the Brabender for a mixing period of approximately 15 minutes. The tensile performance of each sample after compression molding was measured using servo-hydraulic equipment (MTS). Samples were extended at 1 mm/min (original gauge length of 7.62 mm, 13% strain/min) until fracture using a 50 N load cell. Five specimens of each sample were tested.

Sample preparation (pilot scale)

A target formulation was selected based on bench scale measurements, and a large batch of composite material (~100 lbs) was prepared using a corotating twin screw extruder (ZSE 27MAXX, Leistritz) with 12 heating zones. Temperatures along the barrel of the extruder were programmed from 145 ℃ at the inlet to 185 ℃ at the die, with a maximum temperature along the barrel of 190 ℃. The screw speed was set to 110 RPM. Six strands of composite were extruded and pelletized.

Pellets compounded on the twin screw were compression molded following the procedure described above to produce bars according to ASTM D4703, some of which were routed to ASTM D638 Type V dogbones. Pellets were also injection molded using a 35-ton machine (BOY 35 E VV) with 5 heating zones at temperatures ranging from 170-195 ℃. The pellets were plasticized at 300 mm/s to create a 30 mm shot, which was injected into an ASTM D638 Type I dogbone mold using 17 MPa of pressure.

Hexagonal samples were printed using a Big Area Additive Manufacturing (BAAM, Cincinnati Inc) thermoplastic extruder. The BAAM consists of a single screw extruder mounted on a gantry system above a heated bed. Composite pellets were dried at 60 ℃ for 4 hours prior to printing. A polycarbonate build sheet was held in place on the bed with a vacuum system and heated to 60 ℃. The BAAM system consists of 5 heating zones which ranged from 155 to 220 ℃ (feeding zone to nozzle). One to three layers of neat PLA were printed initially to aid in adhesion of the composite to the print bed, after which the feedstock was switched to the composite pellets. Three samples were printed using nozzles with diameters of 0.2” (5.08 mm), 0.3” (7.62 mm), and 0.35” (8.89 mm), respectively. The hexagonal samples were 10” on each side and were printed to a height of at least 8”. The screw speed was set to 30 RPM for each print, and the gantry speed was varied to improve the quality of the extrudate. The layer time during each print was approximately 1 minute.

Characterization (pilot scale)

Differential scanning calorimetry (DSC) measurements were performed on composite pellets and neat PLA using a TA Instruments apparatus. Samples were first equilibrated at 35 ℃, after which they were heated from room temperature to 200 ℃ at 10 ℃/min. samples were then cooled to 35 ℃ and heated again to 200 ℃ at 10 ℃/min. The degree of crystallinity of both samples was calculated using equation 1,

$$X_c = \frac{\Delta H_m - \Delta H_c}{\Delta H_f{}^0 \cdot \varphi} \qquad (1)$$

in which ΔH_m and ΔH_c denote the melting and cold crystallization enthalpies, respectively, of each material, ΔH_f^0 denotes the melting enthalpy of a 100% crystalline PLA sample, and φ denotes the mass fraction of PLA. The value of ΔH_f^0 for PLA was taken as 93 J/g.[9] The melting and cold crystallization enthalpies from the second heating scan were used to calculate the crystallinity of each material.

The thermal degradation of the composite pellets and neat PLA was measured using a TA Instruments thermogravimetric analyzer (TGA). Samples were heated from room temperature to 500 ℃ at 10 ℃/min under argon flow. Measurements were conducted twice for each sample.
The printed hexagons were machined to ASTM D638 Type I dogbones with their axes in the print direction ("x-direction"). The tensile properties of printed and injection molded (IM) samples were tested using a 2 kN load cell at 5 mm/min, while compression molded (CM) samples were tested using a 5 N load cell at 1 mm/min. Five samples of each type were measured.

The viscoelastic response of AM, CM, and IM samples was measuring using dynamic mechanical analysis (DMA, TA Instruments). Samples were clamped with a dual cantilever clamp, and temperature sweeps were performed at a constant frequency of 1 Hz and amplitude within the sample's linear viscoelastic envelope. Each sample was heated from 30 to 120 ℃ at 3 ℃/min. Measurements were conducted twice for each sample type.

The internal structure and porosity of each sample was analyzed using x-ray computed tomography (xCT, Zeiss Metrotom) and VGEasyPore software. Samples were also cut from AM, CM, and IM specimens and potted in cylindrical molds with epoxy. After curing overnight, the samples in epoxy were polished to a mirror finish on a rotating autopolisher (Allied MultiPrep). The samples were then imaged using an optical microscope (Keyence), after which they were sputtered with platinum/palladium and imaged using a scanning electron microscope (SEM, Zeiss Merlin field emission) in secondary electron mode at an accelerating voltage of 1 kV.

Results

Material formulations were first iterated on a small bench scale to find an optimal material for scaling up. PLA with 20 wt.% WF is already a very common AM feedstock, both on large scale system and small desktop printers.[10] In this study, we began formulation work with WF to determine the maximum possible loading in PLA. We then introduced Creafill fibers, which possess a much higher aspect ratio and have better reinforcing potential than WF, in mixtures with the WF. Finally, we tested various additives to the system to improve the melt flow and processability while maintaining as much mechanical performance as possible. As the primary goal of this work was to develop a composite with a high loading of natural fibers that remained processible via AM, the viscoelastic behavior is extremely important in addition to the performance of the resulting material. It was found that samples were unable to be tested using conventional small angle oscillatory rheology, as the high solid content restricted the flow of the material between parallel plates and prohibited relaxation of the normal force on the instrument, meaning the material was unable to reach equilibrium before making a measurement. As such, the torque exerted by the motor of the melt mixing equipment was monitored. As each mixing procedure used identical temperatures and screw speeds, it was inferred that at higher torque

reading was indicative of a higher shear viscosity for qualitative comparison of various formulations.

Bench scale

Samples were first prepared using PLA and WF with 20, 30, 40, and 50% fiber by weight. The samples with 50 wt.% WF were found to be too brittle to successfully remove from the rectangular bar mold after compression molding. As such, all further samples were prepared with 40% fiber by weight. Creafill was then added to the composites at varying ratios of Creafill/WF while maintaining an overall fiber loading of 40 wt.%. The torque during mixing of each sample was monitored on the Brabender instrument, and it was found that increasing the fraction of Creafill directly correlated to increasing torque in the equipment, which can be seen in Figure 1.

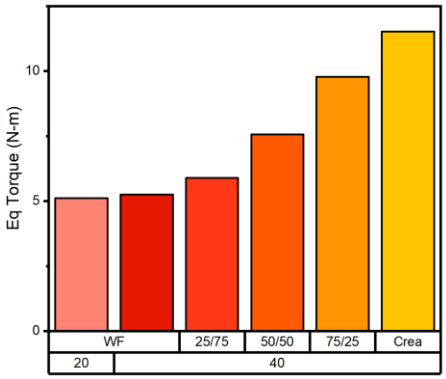

Figure 1. Equilibrium torque (after 15 min) measurements of PLA with 20 and 40 wt.% WF and/or Creafill

PLA with 40 wt.% WF and 40 wt.% Creafill was produced along with 3 mixtures of Creafill and WF at ratios of 25/75, 50/50, and 75/25. Each formulation was compression molded to produce dogbone samples for tensile testing, the results of which are listed in Figure 2.

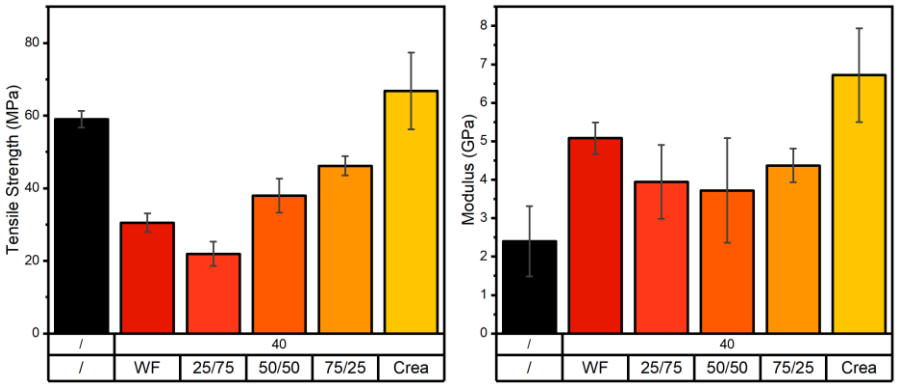

Figure 2. Tensile testing results of PLA with 40 wt.% WF and/or Creafill ("/" refers to neat PLA with no filler)

It is clear from the results in Figure 2 that Creafill is a better reinforcing fiber than WF in terms of tensile performance. Interestingly, the tensile strength and modulus both decreased

slightly upon initial addition of Creafill (25/75 Creafill/WF sample versus 100% WF), but both increased at higher fractions of Creafill in the system. As WF particles have a much lower aspect ratio than Creafill fibers, they can likely flow more easily within a PLA melt in response to a given shear force, while the high aspect ratios of the Creafill fibers could lead to entanglement, increase tortuosity within the melt, and present an overall higher resistance to flow. Based on the above results, a mixture of Creafill and WF at a ratio of 75/25 was chosen for future samples in order to balance the mechanical benefits of Creafill with the processability benefits of WF.

Additives were then selected that had potential to improve the flow behavior of the highly loaded composite while maintaining as much of its mechanical performance as possible. PEG, P(MA-co-E-co-GMA), and a bio-based wax were then melt mixed with PLA and 40 wt.% Creafill/WF (75/25) at 1 wt.% of the additive (59% PLA, 40% fiber, 1% additive by weight).[11, 12] As with previous samples, the torque during mixing was monitored, and the tensile properties of each sample were tested, which are shown in Figures 3 and 4, respectively.

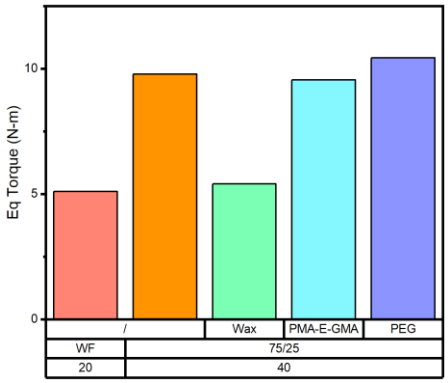

Figure 3. Equilibrium torque measurements of PLA with 20 wt.% WF and 40 wt.% Creafill/WF (75/25) with additives ("/" refers to sample with no additives)

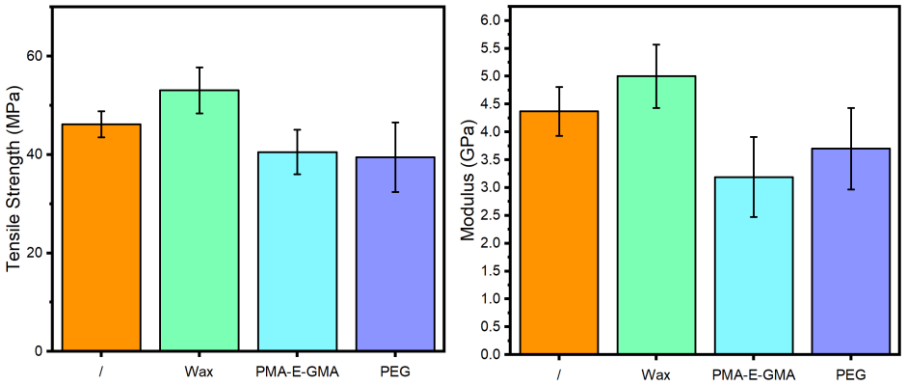

Figure 4. Tensile testing of PLA with 40 wt.% Creafill/WF (75/25) with additives ("/" refers to sample with no additives)

The equilibrium torque of PLA with 20 wt.% WF is given in Figure 3 for reference, as PLA/20 wt.% WF is a common feedstock used in large- and small-scale AM, so its flow behavior was used as a qualitative benchmark in developing a printable highly loaded composite. As can be seen in Figure 3, the addition of wax to the highly loaded mixture significantly decreased its

equilibrium torque, nearly to that exhibited by PLA/20 wt.% WF. Additionally in Figure 4, the addition of wax seems to slightly improve the tensile performance of the composite, although the values measured for tensile strength and modulus were within error of that of the unmodified composite. It was thus decided that PLA with 40 wt.% Creafill/WF (75/25) and 1 wt.% wax would be scaled up for AM trials. Nearly 100 lbs of feedstock was compounded on a twin screw extruder after adjusting the extruder temperatures, pellet and fiber feedrates, and screw speed to maximize extrudate quality and throughput while maintaining the torque on the extruder motor and melt pressure within acceptable ranges (as dictated by the equipment manufacturer).

Pellets compounded on the twin screw extruder were tested for their thermal behavior and stability using DSC and TGA, the results of which are shown in Figure 5. The thermal stability of Creafill and WF was also analyzed by TGA, included in Figure 5.

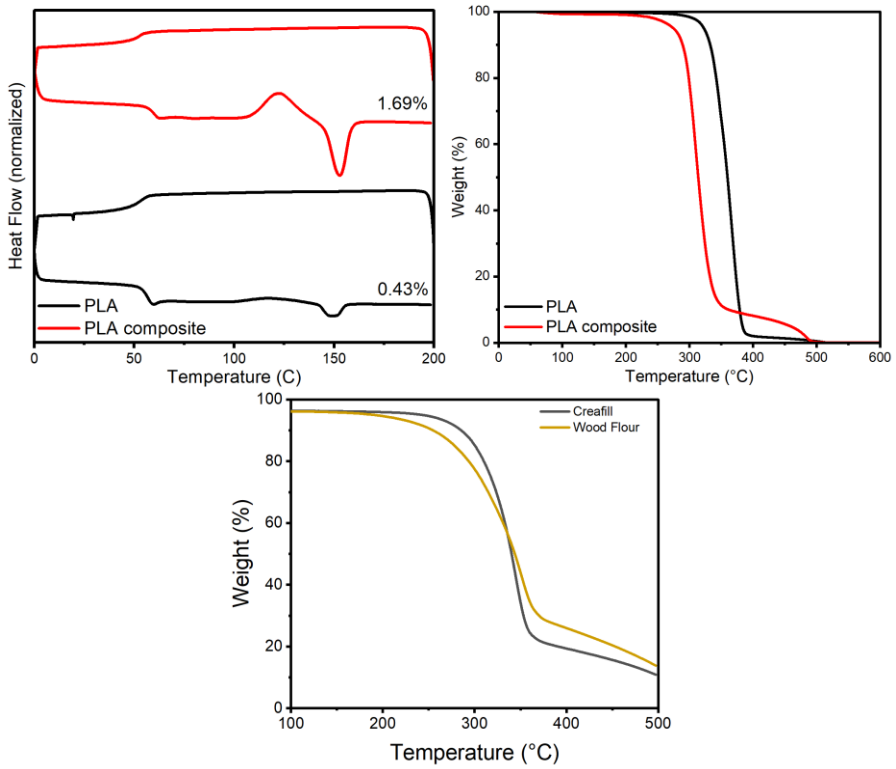

Figure 5. DSC and TGA traces of neat PLA and PLA with 40 wt.% Creafill/WF and 1 wt.% wax and TGA traces of Creafill and WF

As can be seen in the first plot of Figure 5, the incorporation of fibers and wax additives to the PLA matrix significantly increases its cold crystallization and melting enthalpies. The degree of crystallinity within the composite sample was found to be 1.69%, compared to the almost negligible crystallinity within the neat PLA of 0.43%. The glass transition temperature was largely unaffected by the incorporation of fibers and additives to the system. The thermal stability of the material, however, was significantly affected by the addition of fibers and wax. As shown in the second plot of Figure 5, the onset of decomposition in neat PLA was at 337 ℃, while decomposition in the composite sample began at 292 ℃. As can be seen in the last plot of Figure 5, Creafill is more thermally stable than WF, with an onset of degradation at 310 ℃ compared to

WF's 281 ℃. The lower thermal stability of the fibers in the PLA composite undoubtedly were responsible for its decrease in thermal stability in comparison to neat PLA.

Composite pellets were then used to additively manufacture samples using the BAAM at Oak Ridge National Laboratory. The first set of test prints were conducted using a 0.35" diameter nozzle. The initial temperature profile and screw speed were selected based on previous work on the same system with PLA/20 wt.% WF.[10] The torque on the BAAM motor and pressure at the nozzle were observed to be close to the upper limits of the system, so the temperature profile and screw speed were adjusted until a steady, consistent flow could be achieved. Severe sharkskinning was observed initially, which is shown in Figure 6.

Figure 6. Initial AM samples exhibiting sharkskinning and inconsistent flow

The rough appearance of the extruded beads was corrected by iteratively lowering the gantry speed while keeping the screw speed constant (i.e., extruding more material per unit length of printed material). The composite material exhibited very poor adhesion with the polycarbonate build sheet which led to shifting during printing. As such, layers of neat PLA were first printed by hand-feeding PLA pellets into the extruder hopper before filling the hopper with composite pellets. The neat PLA layers can be observed at the base of the left sample in the second image of Figure 6. After parameter optimization, hexagonal samples were printed with three different nozzles with diameters of 0.35", 0.3", and 0.2". An in-process image is shown in Figure 7 along with finished samples.

Figure 7: AM process and printed hexagons

The start/stop region of the hexagons was kept at the same point throughout the print. The material flow became very inconsistent in the start/stop region, likely due to both the composite's high viscosity and the internal settings of the BAAM extruder (gantry and screw are programmed to slow down at a set rate prior to abrupt directional changes/sharp corners), which could likely by overcome with further experimentation. Regardless, the areas affected by inconsistent flow in the start/stop region were discarded from further analysis.

The three hexagons were cut and machined to produce dogbone specimens for tensile testing. Composite pellets were also compression and injection molded to produce tensile dogbones for comparison. Additionally, each sample (3 AM, 1 CM, 1 IM) was analyzed using xCT to image its internal structure and determine its overall volumetric porosity. Images from xCT of each sample are shown in Figure 8, in which black portions within the sample indicate porosity.

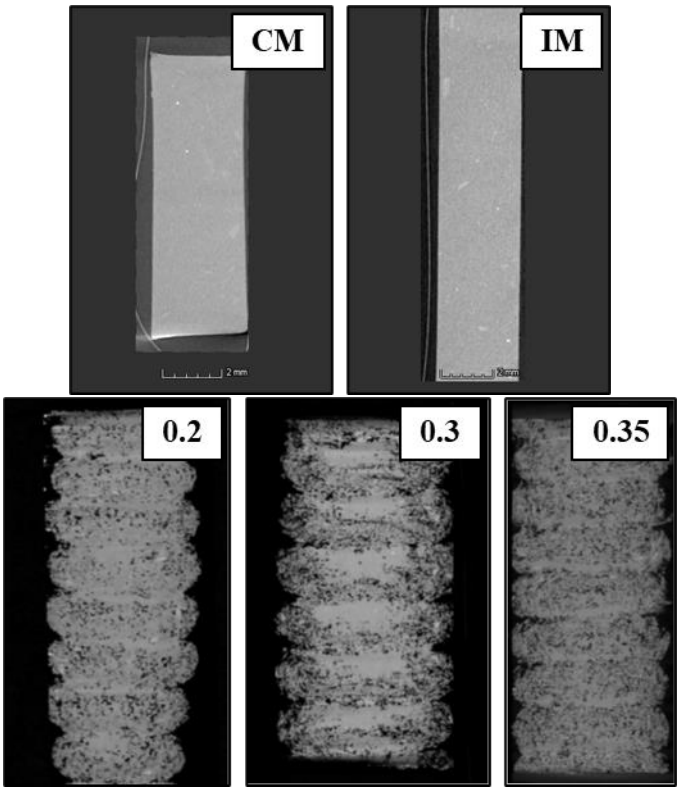

Figure 8. xCT images showing internal structure of CM, IM, and AM samples

It can be clearly seen in Figure 8 that printing introduces a great deal of porosity into the material, while the CM and IM samples are seemingly free of porosity. The volumetric porosity of each sample was quantified and is shown in Figure 9, along with the measured tensile strength of each sample in its print direction.

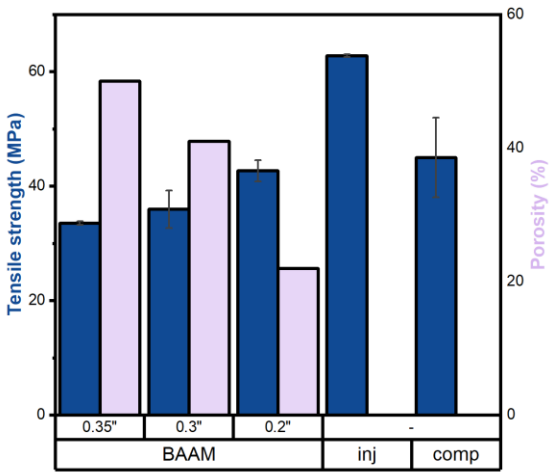

Figure 9. Tensile strength and porosity of AM, IM ("inj"), and CM ("comp") samples

Figure 9 exhibits a clear trend of increasing tensile strength with decreasing porosity. The porosity of samples printed with the 0.35", 0.3", and 0.2" nozzles was found to be 50%, 41%, and 22%, respectively. No porosity was detected in the IM or CM samples. The decrease in porosity with decrease in nozzle size is likely due to the increase in pressure exerted by the smaller nozzles, leading to more compaction or consolidation of the material. Although the IM and CM samples were both nonporous, the tensile strength of the IM sample far exceeded that of the CM sample. This can be attributed to fiber alignment due to the high shear flow within the mold during injection molding.[13] The higher shear exerted by smaller nozzles during AM also likely caused fiber alignment and contributed to the improved tensile performance of the composites, although the positive effects of reduced porosity and fiber alignment are difficult to decouple.[14]

Optical and SEM images of the polished sample surfaces are shown in Figure 10. In the IM and AM samples, the flow direction (flow within the mold or print direction) of the composite during processing is labeled. Fibers can be seen in the higher magnification optical images (appearing white in the images) and SEM images, and there is clear alignment of fibers in each AM and IM sample with the direction of flow. Fibers in the CM sample, however, show no clear directionality. Additionally, macroscale porosity can be seen in the AM samples, labeled with blue arrows in Figure 10. Finally, the different layers of the print in the AM samples can be seen in the low magnification images, reflecting areas of high and low porosity as seen in the xCT images in Figure 8.

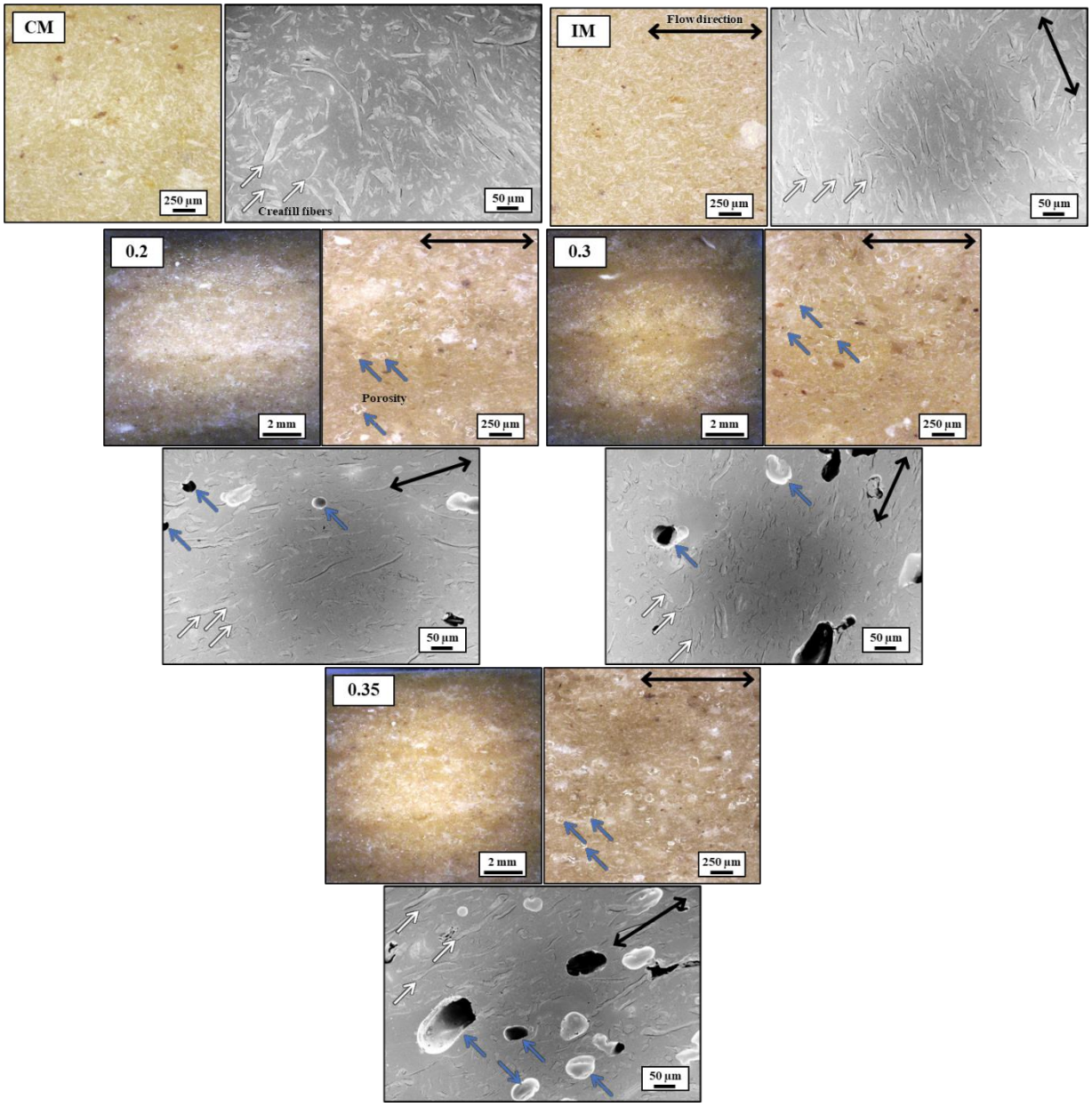

Figure 10. Optical and SEM images of polished surfaces of CM, IM, and AM samples printed with different nozzle sizes. The flow direction on IM and AM samples is labeled with black arrows, porosity is identified by blue arrows, and fibers are identified by white arrows.

Conclusions

A new bio-based feedstock was developed in this work, which sought to reduce the cost of bio-based AM feedstock by increasing the loading of low-cost natural fibers. The PLA used in this work was purchased from NatureWorks at approximately $1.60/lb, while the wood flour and Creafill were obtained at $0.65 and $0.85/lb, respectively. Based on these prices, the typical cost of PLA with 20 wt.% WF is roughly $1.41/lb, while the newly developed feedstock could be obtained at roughly $1.28/lb. Additionally, the embodied energy of the feedstock was also

decreased by increasing the natural fiber content. According to the Eco-Invent database, the embodied energy of PLA is 71.1 MJ/kg, while the embodied energy of bleached Kraft pulp is 46.96 MJ/kg, and the embodied energy of WF can be assumed to be 0, as it is considered a waste material. As such, the embodied energy of PLA with 20% WF is approximately 58.9 MJ/kg, while the embodied energy of the new material in this work is 56.7 MJ/kg. These cost and energy savings could be significant in large or high-volume projects involving tens of thousands of pounds of feedstock. However, these estimates are based on a weighted average of the cost and embodied energies of each constituent material and do not include considerations for packaging, transportation, or drying of materials. The cost and energy of the composite developed in this work could vary greatly depending on the locations of the wood sources, composite production, and processing. Different sources of natural fibers could be considered for similar composites that are local to the composite production and processing site(s), in which case the formulation, processing conditions, and material performance would need to be re-evaluated.

Even more significant was the effect of processing method on the performance of the material, which was shown to be related to both fiber alignment and porosity. The newly developed feedstock, consisting of PLA with 40 wt.% Creafill and WF at a 75/25 ratio, respectively, and 1 wt.% wax, was compounded on a pilot scale system and used to prepare samples using compression and injection molding as well as additive manufacturing on a large format system with three different nozzle sizes. The highest tensile performance was observed in the injection molded sample, followed by the compression molded sample and the three additively manufactured samples in order of increasing nozzle size, meaning the AM samples with the smallest nozzle size showed the best performance. Additive manufacturing with pellet fed systems is known to result in porosity, which can vary based on numerous factors including the size and shape of the pellets, design of the feed system, fiber loading, fiber length, screw/barrel/nozzle design, and processing parameters.[15] It was theorized that porosity induced by AM was responsible for the inferior tensile properties as compared to IM and CM, and the fiber alignment induced by IM led to its higher performance in comparison to the CM samples. The porosity of each sample was visualized using x-ray computed tomography, which proved that the IM and CM samples were virtually free of pores, while the porosity in the AM samples was positively correlated to the nozzle size. Fiber alignment was visualized by potting samples in epoxy and polishing them to a mirror-like finish. The polished samples were then imaged using optical microscopy and SEM. Again, no pores were visible in the IM and CM samples, while porosity was clearly visible in the AM samples. Additionally, alignment of the fibers could be seen in the IM and AM samples, while the fiber orientation appeared random in the CM sample.

Processing methods inducing higher shear and resulting in lower sample porosity resulted in the best mechanical performance of the material developed in this study. To produce materials via AM that could compete with the performance of those produced via IM or CM, the porosity of the material must be reduced. Reducing the nozzle size was shown to decrease part porosity, but reducing the nozzle size results in smaller layers and thinner walls, necessitating more layer and possibly more walls to than printing the same part with a larger nozzle, which can drastically increase print time. However, there are other modifications that could be made to an LFAM system to increase the printed parts' performance. The design of the screw could be changed to impart more shear on the material and alter its compression ratio. Additionally, a vacuum port or vent

could be installed on the extruder to remove volatiles trapped in the barrel during extrusion. This is a very common practice during compounding with twin screw extruders and is known to improve the quality and melt strength of the extrudate. These alterations, among others, would likely result in AM parts with low porosity and highly aligned fibers with mechanical performance rivaling that of injection molded materials.

Acknowledgements

This manuscript has been authored by UT-Battelle, LLC, under contract DE-AC05-00OR22725 with the US Department of Energy (DOE). The authors acknowledge the support from the DOE Office of Energy Efficiency and Renewable Energy, Advanced Materials and Manufacturing Technologies Office, and the Oak Ridge National Laboratory/University of Maine Hub & Spoke Program team. Microscopy studies were completed at the Center for Nanophase Materials Sciences, a DOE Office of Science User Facility. The US government retains and the publisher, by accepting the article for publication, acknowledges that the US government retains a nonexclusive, paid-up, irrevocable, worldwide license to publish or reproduce the published form of this manuscript, or allow others to do so, for US government purposes. DOE will provide public access to these results of federally sponsored research in accordance with the DOE Public Access Plan (https://www.energy.gov/doe-public-access-plan).

References

[1] S. M. E. Sepasgozar, A. Shi, L. Yang, S. Shirowzhan, and D. J. Edwards, "Additive Manufacturing Applications for Industry 4.0: A Systematic Critical Review," *Buildings*, vol. 10, no. 12, 2020, doi: 10.3390/buildings10120231.

[2] H. Storz and K. Vorlop, "Bio-based plastics: status, challenges, and trends," *Landbauforschung Völkenrode*, vol. 63, pp. 321-332, 2013, doi: 10.3220/LBF_2013_321-332.

[3] A. R. Torrado Perez, D. A. Roberson, and R. B. Wicker, "Fracture Surface Analysis of 3D-Printed Tensile Specimens of Novel ABS-Based Materials," *Journal of Failure Analysis and Prevention*, vol. 14, no. 3, pp. 343-353, 2014, doi: 10.1007/s11668-014-9803-9.

[4] L. Love *et al.*, "The importance of carbon fiber to polymer additive manufacturing," *Journal of Materials Research*, vol. 29, no. 17, 2014.

[5] S. Pilla, S. Gong, E. O'Neill, R. M. Rowell, and A. M. Krzysik, "Polylactide-pine wood flour composites," (in English), *Polym Eng Sci*, vol. 48, no. 3, pp. 578-587, Mar 2008, doi: 10.1002/pen.20971.

[6] Y. Huang, S. Löschke, and G. Proust, "In the mix: The effect of wood composition on the 3D printability and mechanical performance of wood-plastic composites," *Composites Part C: Open Access*, vol. 5, 2021, doi: 10.1016/j.jcomc.2021.100140.

[7] N. Ayrilmis, M. Kariž, and M. Kitek Kuzman, "Effect of wood flour content on surface properties of 3D printed materials produced from wood flour/PLA filament," *International Journal of Polymer Analysis and Characterization*, vol. 24, no. 7, pp. 659-666, 2019, doi: 10.1080/1023666x.2019.1651547.

[8] K. K. Sadasivuni, P. Saha, J. Adhikari, K. Deshmukh, M. B. Ahamed, and J. J. Cabibihan, "Recent advances in mechanical properties of biopolymer composites: a review," *Polymer Composites*, vol. 41, no. 1, pp. 32-59, 2019, doi: 10.1002/pc.25356.

[9] E. W. Fischer, H. J. Sterzel, and G. Wegner, "Investigation of the structure of solution grown crystals of lactide copolymers by means of chemical reactions," *Kolloid-Zeitschrift und Zeitschrift fur Polymere*, vol. 251, pp. 980-990, 1973.

[10] K. Copenhaver *et al.*, "Recyclability of additively manufactured bio-based composites," *Composites Part B: Engineering,* vol. 255, 2023, doi: 10.1016/j.compositesb.2023.110617.
[11] F.-J. Li, L.-C. Tan, S.-D. Zhang, and B. Zhu, "Compatibility, steady and dynamic rheological behaviors of polylactide/poly(ethylene glycol) blends," *Journal of Applied Polymer Science,* vol. 133, no. 4, pp. n/a-n/a, 2016, doi: 10.1002/app.42919.
[12] M. Wang, X. Liang, H. Wu, L. Huang, and G. Jin, "Super toughed poly (lactic acid)/poly (ethylene vinyl acetate) blends compatibilized by ethylene-methyl acrylate-glycidyl methacrylate copolymer," *Polymer Degradation and Stability,* vol. 193, 2021, doi: 10.1016/j.polymdegradstab.2021.109705.
[13] C. S. Kanjanaphorn Chansoda, Watcharapong Chookaew, "Comparative study on the wood-based PLA fabricated by compression molding and additive manufacturing," presented at the The 11th International Conference on Mechanical Engineering, 2021.
[14] N. S. Hmeidat, R. C. Pack, S. J. Talley, R. B. Moore, and B. G. Compton, "Mechanical anisotropy in polymer composites produced by material extrusion additive manufacturing," *Additive Manufacturing,* vol. 34, 2020, doi: 10.1016/j.addma.2020.101385.
[15] X. Wang, L. Zhao, J. Y. H. Fuh, and H. P. Lee, "Effect of Porosity on Mechanical Properties of 3D Printed Polymers: Experiments and Micromechanical Modeling Based on X-ray Computed Tomography Analysis," *Polymers (Basel),* vol. 11, no. 7, Jul 5 2019, doi: 10.3390/polym11071154.